Therefore, in the present study we investigated the relationships between various fat parameters, including VFA, and early surgical outcomes following gastrectomy to clarify the most appropriate fat parameter to predict the development of pancreas-related infection and anastomotic leakage.

Methods

Patients

Between April 2008 and March 2009, a total of 217 patients underwent open distal or total gastrectomy with curative intent for primary gastric cancer at Shizuoka Cancer Center, Shizuoka, Japan. Patients who underwent splenectomy, distal pancreatic resection, and cholecystectomy were included in the study, whereas seven patients who underwent combined resection of other organs (liver, colon, and adrenal gland) and four patients who had synchronous cancer in other organs (colon, rectum, and kidney) were excluded from the study. Therefore, data from 206 patients were analyzed in the present study.

Lymph node station number, the degree of lymph node dissection, and pathological stage were determined on the basis of the *Japanese classification of gastric carcinoma* [15] and the *Gastric cancer treatment guidelines in Japan* [16]. Gastrectomy with D2 lymph node dissection was performed in patients with advanced gastric cancer, whereas D1 plus beta lymph node dissection (i.e., D1 + numbers 7, 8a, 9) was performed in patients with early gastric cancer.

Fat measurement

Multidetector computed tomography (MDCT) was performed in all patients prior to surgery. Patients were examined while in the supine position, with their arms stretched above their heads, at the end of inspiration, using a CT scanner (Aquilion; Toshiba Medical Systems, Tokyo, Japan). Parameters for scanning were: tube voltage, 120 kVp; scan time, 0.5 s; and reconstruction slice thickness, 2 mm. The tube current was determined automatically by the CT automatic exposure control system. The images obtained were transferred to a Ziostation workstation (Ziosoft, Tokyo, Japan), which was used to quantify the total fat area (TFA), subcutaneous fat area (SFA), and VFA at the level of the umbilicus. In the present study, relationships between early surgical outcomes following gastrectomy and TFA, VFA, SFA, and BMI, as the fat parameters, were investigated.

Definition of early surgical outcomes

Operating time, intraoperative blood loss, the number of lymph nodes retrieved, postoperative morbidity and mortality, and the duration of the postoperative hospital stay were investigated as early surgical outcomes.

Patients with Grade II or greater complications based on the Clavien-Dindo classification were defined as having postoperative morbidity [17]. In the present study, pancreas-related infection was diagnosed on the basis of the definitions of the International Study Group on Pancreatic Fistula (ISGPF) [18]. Diagnosis of anastomotic leakage was confirmed by radiological examination using contrast media. Postoperative mortality was defined as any death within 30 postoperative days (PODs).

Statistical analysis

Spearman's rank correlation coefficient was used to evaluate relationships between individual fat parameters (BMI, TFA, SFA, and VFA) and early surgical outcomes (operating time, intraoperative blood loss, number of lymph nodes retrieved, postoperative hospital stay). Relationships between individual fat parameters and the categorical variables of pancreas-related infection and anastomotic leakage were evaluated using logistic regression.

To identify independent risk factors for each of the intra-abdominal infectious complications, a multivariate logistic regression model with forward selection was used, with BMI, TFA, SFA, VFA, age, sex, operating time, intraoperative blood loss, number of lymph nodes retrieved, surgical procedure (total or distal gastrectomy), type of lymph node dissection (D2 or D1 plus beta), and splenectomy (yes or no) included as covariates.

All statistical analyses were performed using SPSS version 13.0 (SPSS, Chicago, IL, USA). All continuous data are presented as medians (ranges). $P < 0.05$ was considered significant.

Results

Patients' characteristics

The patients' characteristics are given in Table 1. Total gastrectomy was performed in 48 patients, 29 of whom also underwent splenectomy for the removal of splenic hilar lymph nodes. Additional pancreatosplenectomy was performed in 2 of the 48 patients. The remaining 158 patients underwent distal gastrectomy. D2 lymph node dissection was performed in 111 patients, whereas 95 patients underwent D1 plus beta lymph node dissection.

Table 2 lists the early surgical outcomes of all patients. Postoperative complications were observed in 55 patients (26.7%). The incidence of pancreas-related infection and anastomotic leakage was 8.7% and 4.9%, respectively. Five patients had both pancreas-related infection and

Table 1 Clinocopathological characteristics of patients

Age (years)	65.9 (39–89)
Sex (male/female)	146/60
Diabetes mellitus (*n*)	17
Individual fat parameter	
BMI (kg/m^2)	23 (16.0–32.3)
TFA (cm^2)	198 (6.9–505.8)
SFA (cm^2)	107.4 (3.0–266.9)
VFA (cm^2)	90.5 (3.6–262.5)
Surgical procedure (*n*)	
Total gastrectomy	48
Distal gastrectomy	158
Lymph node dissection (*n*)	
D2	111
D1 plus beta	95
Splenectomy (*n*)	
Yes	29
No	177
Pathological stage (*n*)	
IA	88
IB	48
II	44
IIIA	15
IIIB	9
IV	2

Unless indicated otherwise, values are means, with ranges given in parentheses

BMI body mass index, *TFA* total fat area, *SFA* subcutaneous fat area, *VFA* visceral fat area

Table 2 Early surgical outcomes of 206 patients

Operating time (min)	194 (103–489)
Intraoperative blood loss (mL)	265 (13–2606)
No. of lymph nodes retrieved	37 (8–109)
Postoperative complications	55 (26.7%)
Pancreas-related infection	18 (8.7%)
Anastomotic leakage	10 (4.9%)
Postoperative hospital deaths	1 (0.5%)
Duration of postoperative hospital stay (days)	11 (7–87)

Values are presented as either median with ranges in parentheses or as the number of patients in each group, with percentages in parentheses

anastomotic leakage. Both of the two patients who underwent distal pancreatectomy had pancreas-related infection. Postoperative mortality was observed in one patient (0.5%). This patient had undergone distal gastrectomy with D2 lymph node dissection, and anastomotic leakage developed on POD 7. This patient died suddenly on POD 9 due to a pulmonary embolism.

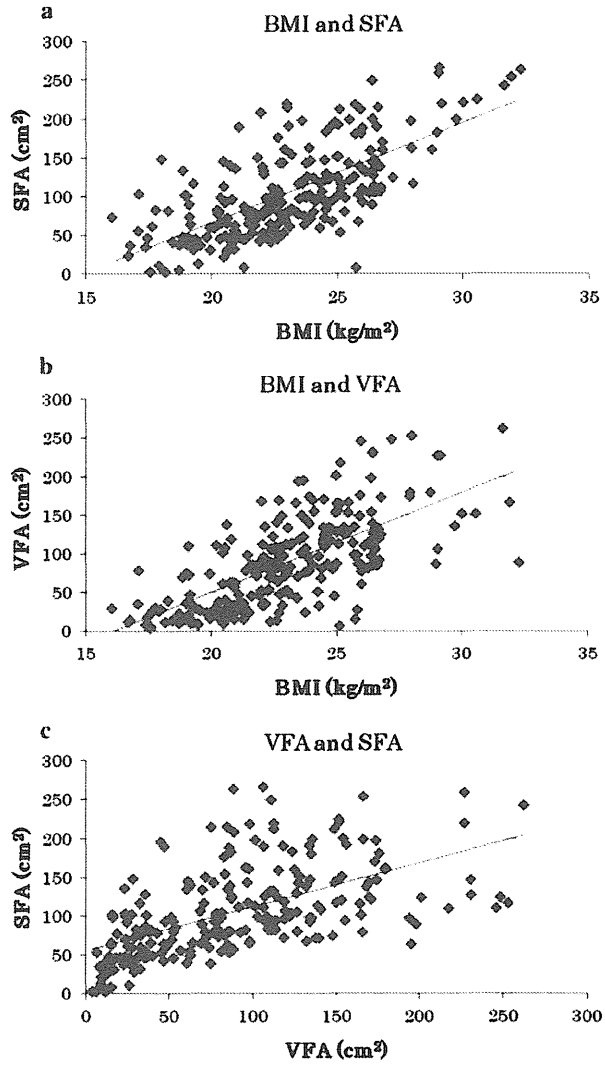

Fig. 1 Correlations between **a** superficial fat area (*SFA*) and body mass index (*BMI*); $R = 0.672$, $P < 0.001$, **b** visceral fat area (*VFA*) and BMI; $R = 0.683$, $P < 0.001$, and **c** SFA and VFA; $R = 0.555$, $P < 0.001$. Significant associations were observed for all comparisons

Relationships between fat parameters and early surgical outcomes

Figure 1 shows the correlations between SFA, VFA, and BMI. Significant correlations were found between SFA and both BMI and VFA, as well as between VFA and BMI. Correlation coefficients for each of the fat parameters and operating time, intraoperative blood loss, number of lymph nodes retrieved, and postoperative hospital stay are given in Table 3. Although VFA was weakly associated with prolonged operating time (correlation coefficient 0.304) and increased intraoperative blood loss (correlation coefficient 0.371), no significant relationships were observed for any of the fat parameters and operation time,

Table 3 Relationship between fat parameters and early surgical outcome data

	Intraoperative blood loss	Operating time	No. of lymph nodes retrieved	Postoperative hospital stay
BMI	0.295 (<0.001)	0.235 (0.001)	−0.196 (0.005)	0.011 (0.872)
TFA	0.322 (<0.001)	0.250 (<0.001)	−0.134 (0.055)	0.103 (0.139)
SFA	0.199 (0.004)	0.153 (0.028)	−0.022 (0.756)	0.025 (0.726)
VFA	0.371 (<0.001)	0.304 (<0.001)	−0.197 (0.005)	0.155 (0.026)

Values are the correlation coefficients, with *P* values given in parentheses

BMI body mass index, *TFA* total fat area, *SFA* subcutaneous fat area, *VFA* visceral fat area

Table 4 Identification of risk factors for the development of pancreas-related infection and anastomotic leakage, determined using univariate analysis

	Pancreas-related infection			Anastomotic leakage		
	Odds ratio	95% CI	*P*	Odds ratio	95% CI	*P*
BMI (kg/m^2)	1.318	1.121–1.548	0.001	1.156	0.946–1.411	0.156
TFA (cm^2)	1.009	1.004–1.014	0.001	1.003	0.997–1.009	0.291
SFA (cm^2)	1.008	1.001–1.016	0.035	0.999	0.987–1.010	0.802
VFA (cm^2)	1.016	1.008–1.025	0.001	1.010	1.000–1.021	0.042
Age (years)	0.978	0.934–1.023	0.332	0.997	0.937–1.061	0.923
Sex (male or female)	2.335	0.655–8.323	0.191	1.681	0.346–8.158	0.519
Intraoperative blood loss (mL)	1.002	1.001–1.003	0.001	1.001	1.000–1.002	0.227
Operating time (min)	1.010	1.003–1.018	0.007	1.006	0.996–1.016	0.234
No. of lymph nodes retrieved	0.987	0.954–1.021	0.458	0.961	0.912–1.012	0.133
Surgical procedure (total or distal)	5.574	2.094–14.841	0.001	2.303	0.622–8.526	0.212
Lymph node dissection (D2 or D1)	3.555	1.137–11.110	0.029	1.300	0.356–4.751	0.692
Splenectomy (yes or no)	7.515	2.729–20.694	0.001	0.667	0.081–5.468	0.706

CI confidence interval, *BMI* body mass index, *TFA* total fat area, *SFA* subcutaneous fat area, *VFA* visceral fat area

intraoperative blood loss, the number of lymph nodes retrieved, or the duration of the postoperative hospital stay.

Risk factors for intra-abdominal infectious complications

Tables 4 and 5 list the results of univariate and multivariate analyses used to identify risk factors for intra-abdominal infectious complications. On the basis of the univariate analysis, all fat parameters, operating time, intraoperative blood loss, surgical procedure, type of lymph node dissection, and splenectomy affected the development of pancreas-related infection. Multivariate analysis revealed that VFA, intraoperative blood loss, and splenectomy were independent risk factors for pancreas-related infection, with odds ratios (95% confidence intervals) of 1.015 (1.005–1.025), 1.001 (1.000–1.003), and 7.125 (2.083–24.372), respectively. With regard to anastomotic leakage, both univariate and multivariate analyses revealed VFA as a risk factor for the development of anastomotic leakage, with an odds ratio (95% confidence interval) on multivariate analysis of 1.010 (1.000–1.021).

Table 5 Multivariate analysis identification of independent risk factors for the development of pancreas-related infection

	Odds ratio	95% CI	*P*
VFA (cm^2)	1.015	1.005–1.025	0.004
Intraoperative blood loss (mL)	1.001	1.000–1.003	0.009
Splenectomy (yes or no)	7.125	2.083–24.372	0.002

CI confidence interval, *VFA* visceral fat area

In order to justify the use of correlation analysis to find risk factors for the surgical complications, it was mandatory to prove that the fat components did not relate to outcomes in binomial fashion. To do so, we divided the patients into 4 groups according to the VFA (<35.8, 35.8–85.6, 85.6–126.5, and >126.5 cm^2), and looked at the incidence of surgical complications in each group. Pancreas-related complications were observed in 0, 2, 8, and 8 patients, respectively, in these 4 groups, showing that the relationship between VFA and surgical complications was not binomial.

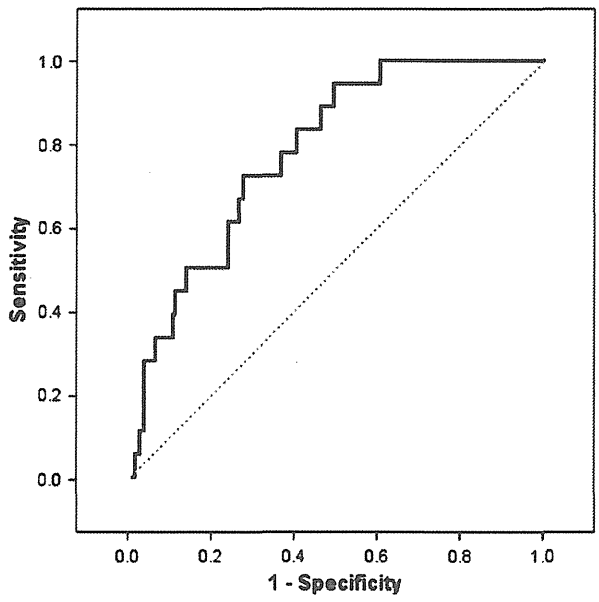

Fig. 2 Receiver operating characteristic (ROC) curve to identify the appropriate cut-off value of VFA to predict pancreas-related infection. The area under the curve (AUC) was 0.787 and the threshold of VFA was 113.6 cm^3 with sensitivity of 72.2% and specificity of 62.9%

The cut-off value for VFA as an indicator of pancreas-related infection

Figure 2 shows the receiver operating characteristic (ROC) curve used to identify the appropriate cut-off value of VFA to predict pancreas-related infection. The area under the curve (AUC) was 0.787 and the threshold of VFA was 113.6 cm^2 with sensitivity of 72.2% and specificity of 62.9%.

Discussion

The incidence of postoperative morbidity following gastrectomy with lymph node dissection (D2 or more) has been reported to be 17–21% in eastern Asia [19, 20] and 21–46% in Europe [3, 4, 21–25]. Previous studies of the risk factors for postoperative morbidity indicate that obesity, defined as BMI > 25 kg/m^2, is one of the most important [8–10]. The recent development of specific computer software has enabled the easy calculation of the amount of visceral fat, and some authors have suggested that the VFA may be a better predictor of the development of postoperative morbidity than the BMI [13, 14].

Of all morbidities, intra-abdominal infectious complications, including pancreas-related infection and anastomotic leakage, are potentially fatal complications; thus, in the present study, we investigated independent risk factors for both of these complications. Although Tokunaga et al. [13] have reported that excessive visceral fat is a risk factor for postoperative intra-abdominal infectious complications and Tanaka et al. [14] have reported that the amount of visceral fat affects the development of pancreas-related infection, independent risk factors for both complications had not been investigated simultaneously in previous studies. In the present study, we determined the factors affecting the development of both pancreas-related infection and anastomotic leakage.

The results of the present study indicate that a high VFA is associated with the development of both pancreas-related infection and anastomotic leakage following gastrectomy. To date, the risk factors for anastomotic leakage after gastrectomy have not been completely clarified [26]. Both Ser et al. [27] and Kang et al. [28] have reported that anastomotic leakage may occur in cases in which there is excess tension and pressure on the anastomotic site and that these conditions are more frequently observed in patients with excessive visceral fat because the thick mesentery creates tension on the anastomosis. In addition, a deeper surgical field in these patients, and preoperative comorbidities, such as cardiovascular disease or diabetes mellitus, which are frequently seen in obese patients, may affect the development of anastomotic leakage [29–31].

In the present study, pancreas-related infections were observed in 18 patients (8.7%), with splenectomy, intraoperative blood loss, and VFA identified as independent risk factors. Splenectomy is a well-known and widely accepted risk factor, because manipulation of the tail of the pancreas during the procedure increases the risk of pancreas-related infection [6, 14, 31]. In Europe, the final results of the Dutch D1D2 trial recommended D2 gastrectomy. However, they also recommended that the spleen should be preserved, because of increased morbidity and mortality after splenectomy [32]. In Japan, though the current standard treatment for upper-third gastric cancer is a total gastrectomy with splenectomy, a recent randomized controlled trial revealed a high incidence of postoperative complications after splenectomy [33]. We should await final survival analysis of this study before we conclude whether or not the spleen has to be preserved. Distal pancreatectomy has been thought to be correlated with pancreas-related complications. In the present study, actually, both of the two patients with pancreatectomy had this complication. However, the number was so small that further analysis could not be done.

In the present study, excessive visceral fat also increased the incidence of pancreas-related infection. It has been proposed that excessive visceral fat makes it difficult to find the border between the pancreas and lymph nodes, which may result in intraoperative pancreatic injury [13, 14]. Our ROC analysis revealed that a VFA of 113.6 cm^2

was an appropriate cut-off value. Careful surgery will be required particularly in these patients having a VFA of 113.6 cm^2 or more.

Although the present study identified a significant relationship between intraoperative blood loss and pancreas-related infection, others have reported that increased bleeding does not affect the incidence of pancreas-related infection [34, 35]. We believe that increased bleeding may have created difficulties in identifying the border between the pancreas and lymph nodes, as occurs in patients with excessive visceral fat, thus contributing to an increased incidence of pancreas-related infection.

Preoperative co-morbidities have also been considered to affect the incidence of postoperative complications. Also, poor nutritional status due to advanced primary gastric cancer may be associated with a high incidence of postoperative complications. However, in the present study, the patients' preoperative nutritional status (performance status, serum albumin level) and co-morbidities (diabetes mellitus, hypertension) were not associated with the incidence of intra-abdominal infectious complications (data not shown).

In conclusion, excessive visceral fat, represented by the VFA, was found to be an independent risk factor for both pancreas-related infection and anastomotic leakage following gastrectomy. Greater diligence during surgery is necessary for patients with excessive visceral fat, particularly if splenectomy has to be performed simultaneously.

References

1. Maruyama K, Okabayashi K, Kinoshita T. Progress in gastric cancer surgery in Japan and its limits of radicality. World J Surg. 1987;11:418–25.
2. Sasako M, McCulloch P, Kinoshita T, Maruyama K. New method to evaluate the therapeutic value of lymph node dissection for advanced gastric cancer. Br J Surg. 1995;82:346–51.
3. Bonenkamp JJ, Songun I, Hermans J, Sasako M, Welvaart K, Plukker JTM, et al. Randomised comparison of morbidity after D1 and D2 dissection for gastric cancer in 996 Dutch patients. Lancet. 1995;2345:745–8.
4. Cuschieri A, Fayers P, Fielding J, Craven J, Bancewicz J, Joypaul V, et al. Postoperative morbidity and mortality after D1 and D2 resections for gastric cancer: preliminary results of the MRC randomised controlled surgical trial. Lancet. 1996;347:995–9.
5. Bonekamp JJ, Hermans J, Sasako M, van de Velde CJH. Extend lymph-node dissection for gastric cancer. N Engl J Med. 1999;340:908–14.
6. Cuschieri A, Weeden S, Fielding J, Bancewicz J, Craven J, Joypaul V, et al. Patient survival after D1 and D2 resections for gastric cancer: long-term results of the MRC randomized surgical trial. Surgical Co-operative Group. Br J Cancer. 1999;79: 1522–30.
7. Kubo M, Sano T, Fukagawa T, Katai H, Sasako M. Increasing body mass index in Japanese patients with gastric cancer. Gastric Cancer. 2005;8:39–41.
8. Inagawa S, Adachi S, Oda T, Kawamoto T, Koike N, Fukao K. Effect of fat volume on postoperative complications and survival rate after D2 dissection for gastric cancer. Gastric Cancer. 2000;3:141–4.
9. Tsujinaka T, Sasako M, Yamamoto S, Sano T, Kurokawa Y, Nashimoto A, et al. Influence of overweight on surgical complications for gastric cancer: results from a randomized control trial comparing D2 and extended paraaortic D3 lymphadenectomy (JCOG9501). Ann Surg Oncol. 2007;14:355–61.
10. Ojima T, Iwahashi M, Nakamori M, Nakamura M, Naka T, Ishida K, et al. Influence of overweight on patients with gastric cancer after undergoing curative gastrectomy. Arch Surg. 2009;144(4): 351–8.
11. Gretschel S, Christoph F, Bembenek A, Estevez-Schwarz L, Schneider U, Schlag PM. Body mass index does not affect systematic D2 lymph node dissection and postoperative morbidity in gastric cancer patients. Ann Surg Oncol. 2003;10:363–8.
12. Lee JH, Paik YH, Lee JS, Ryu KW, Kim CG, Park SR, et al. Abdominal shape of gastric cancer patients influences short-term surgical outcomes. Ann Surg Oncol. 2007;14:1288–94.
13. Tokunaga M, Hiki N, Fukunaga T, Ogura T, Miyata S, Yamaguchi T. Effect of individual fat areas on early surgical outcomes after open gastrectomy for gastric cancer. Br J Surg. 2009; 96:496–500.
14. Tanaka K, Miyashiro I, Yano M, Kishi K, Motoori M, Seki Y, et al. Accumulation of excess visceral fat is a risk factor for pancreatic fistula formation after total gastrectomy. Ann Surg Oncol. 2009;16:1520–5.
15. Japanese Gastric Cancer Association. Japanese classification of gastric carcinoma—2nd English edition. Gastric Cancer. 1998;1: 10–24.
16. Nakajima T. Gastric cancer treatment guidelines in Japan. Gastric Cancer. 2002;5:1–5.
17. Dindo D, Demartines N, Clavien PA. Classification of surgical complications. A new proposal with evaluation in a cohort of 6336 patients and results of a survey. Ann Surg. 2004;240: 205–13.
18. Bassi C, Dervenis C, Butturini G, Fingerhut A, Yeo C, Izbicki J, et al. Postoperative pancreatic fistula: an international study group (ISGPF) definition. Surgery. 2005;138:8–13.
19. Sano T, Sasako M, Yamamoto S, Nashimoto A, Kurita A, Hiratsuka M, et al. Gastric cancer surgery: morbidity and mortality results from a prospective randomized controlled trial comparing D2 and extended para-aortic lymphadenectomy—Japan Clinical Oncology Group Study 9501. J Clin Oncol. 2004;22:2767–73.
20. Wu CW, Hsiung CA, Lo SS, Hsieh MC, Shia LT, Whang-Peng J. Randomized clinical trial of morbidity after D1 and D3 surgery for gastric cancer. Br J Surg. 2004;91:283–7.
21. de Manzoni G, Verlato G, Guglielmi A, Laterza E, Genna M, Cordiano C. Prognostic significance of lymph node dissection in gastric cancer. Br J Surg. 1996;83:1604–7.
22. Smith BR, Stabile BE. Aggressive D2 lymphadenectomy is required for accurate pathologic staging of gastric adenocarcinoma. Am Surg. 2006;72:849–52.
23. Marrelli D, Pedrazzani C, Neri A, Corso G, DeStefano A, Pinto E, et al. Complications after extended (D2) and superextended (D3) lymphadenectomy for gastric cancer: analysis of potential risk factors. Ann Surg Oncol. 2007;14:25–33.
24. Danielson H, Kokkola A, Kiviluoto T, Siren J, Luohimo J, Kivilaakso E, et al. Clinical outcome after D1 vs D2–3 gastrectomy for treatment of gastric cancer. Scand J Surg. 2007;96:35–40.
25. Degiuli M, Sasako M, Ponti A, Calvo F. Survival results of a multicentre phase II study to evaluate D2 gastrectomy for gastric cancer. Br J Cancer. 2004;90:1727–32.
26. Sierzega M, Kolodziejczyk J, Kulig J, Polish Gastric Cancer Study Group. Impact of anastomotic leakage on long-term

survival after total gastrectomy for carcinoma of the stomach. Br J Surg. 2010;97:1035–42.
27. Ser KH, Lee WJ, Lee YC, et al. Experience in laparoscopic sleeve gastrectomy for morbidly obese Taiwanese: staple-line reinforcement is important for preventing leakage. Surg Endosc. 2010;24:2253–9.
28. Kang KC, Cho GS, Han SU, Kim W, Kim HH, Kim MC, et al. Comparison of Billroth I and Billroth II reconstructions after laparoscopy-assisted distal gastrectomy: a retrospective analysis of large-scale multicenter results from Korea. Surg Endosc. 2011;25:1953–61.
29. Grotenhuis BA, Wijnhoven BPL, Hötte GJ, van der Stok EP, Tilanus HW, van Lanshot JJB, et al. Prognostic value of body mass index on short-term and long-term outcome after resection of esophageal cancer. World J Surg. 2010;34:2621–7.
30. Pi-Sunyer FX. Medical hazards of obesity. Ann Intern Med. 1993;119:655–60.
31. Despres JP, Lemieux I. Abdominal obesity and metabolic syndrome. Nature. 2006;444:881–7.
32. Songun I, Putter H, Kranenbarg EM, Sasako M, Van de Velde CJ. Surgical treatment of gastric cancer: 15-year follow-up results of the randomised nationwide Dutch D1D2 trial. Lancet Oncol. 2010;11:439–49.
33. Sano T, Sasako M, Shibata T, Yamamoto S, Tsuburaya A, Nashimoto A, et al. Randomized controlled trial to evaluate splenectomy in total gastrectomy for proximal gastric carcinoma (JCOG0110): Analyses of operative morbidity, operation time, and blood loss. J Clin Oncol 2010;28:15s (suppl; abstr 4020).
34. Katai H, Yoshimura K, Fukagawa T, Sano T, Sasako M. Risk factors for pancreas-related abscess after gastrectomy. Gastric Cancer. 2005;8:137–41.
35. Nobuoka D, Gothda N, Konishi M, Nakagohri T, Takahashi S, Kinoshita T. Prevention of postoperative pancreatic fistula after total gastrectomy. World J Surg. 2008;32:2261–6.

Gastric Cancer (2012) 15:144–153
DOI 10.1007/s10120-011-0090-9

ORIGINAL ARTICLE

$CD83^+$ dendritic cells and $Foxp3^+$ regulatory T cells in primary lesions and regional lymph nodes are inversely correlated with prognosis of gastric cancer

Seigo Kashimura · Zenichiro Saze · Masanori Terashima · Nobutoshi Soeta · Satoshi Ohtani · Fumihiko Osuka · Michihiko Kogure · Mitsukazu Gotoh

Received: 25 April 2011 / Accepted: 11 August 2011 / Published online: 15 November 2011

Abstract
Background Dendritic cells (DCs) are potent antigen-presenting cells that are central to the regulation, maturation, and maintenance of the cellular immune response against cancer. In contrast, $CD4^+CD25^+$ regulatory T cells (Tregs) play a central role in self-tolerance and suppress antitumor immunity. In this study, we investigated the clinical significance of mature $CD83^+$ DCs and $Foxp3^+$ Tregs in the primary tumor and regional lymph nodes from the viewpoint of the two opposing players in the immune responses.
Methods We investigated, immunohistochemically, the density of $CD83^+$ DCs and $Foxp3^+$ Tregs in primary lesions of gastric cancer ($n = 123$), as well as in regional lymph nodes with ($n = 40$) or without metastasis ($n = 40$).
Results Decreased density of $CD83^+$ DCs and increased density of $Foxp3^+$ Tregs were observed in the primary tumor and metastatic lymph nodes. Density was significantly correlated with certain clinicopathological features. Poor prognosis was observed in patients with a low density of $CD83^+$ DCs and a high density of $Foxp3^+$ Tregs in primary lesions. For patients with metastatic lymph nodes, the density of $CD83^+$ DCs in negative lymph nodes was found to be an independent prognostic factor by multivariate analysis.
Conclusion The density of $CD83^+$ DCs and $Foxp3^+$ Tregs was inversely correlated with tumor progression and reflected the prognosis of gastric cancer.

Keywords Gastric cancer · Dendritic cells · Regulatory T cells · Prognosis

Introduction

Dendritic cells (DCs), as professional antigen-presenting cells (APCs), play an important role in the antitumor immune response. DCs take up tumor-associated antigen in tumor tissue and migrate to regional lymph nodes to generate cytotoxic T cells. The antigen/pathogen induces the immature DCs to undergo phenotypic and functional changes that culminate in the complete transition from antigen-capturing cells to APCs. DC maturation is intimately linked with their migration from the peripheral tissue to the draining lymphoid organs [1]. CD83 is a 45-kDa transmembranous protein and member of the immunoglobulin super family [2], and is expressed by mature DCs, but not by B cells, natural killer (NK) cells, or monocytes [3], and can be a useful marker of mature DCs [4–6]. Previous studies have shown that a low density of $CD83^+$ DCs in various cancer tissues is associated with poor prognosis [7–12]. However, regarding DC activation, it is not clear what kind of immune responses occur in the draining lymph nodes.

In contrast to the activation of immune responses initiated by DCs, the immune response in tumors is suppressed by $CD4^+CD25^+$ regulatory cells (Tregs) [13–16], which play an important role in immunological self-tolerance [17, 18]. Tregs have also been shown to contribute to cancer-related immunosuppression [19, 20]. Recently, it has been reported that Foxp3, forkhead/winged helix transcription

S. Kashimura · Z. Saze · N. Soeta · S. Ohtani · F. Osuka · M. Kogure · M. Gotoh (✉)
Department of Surgery I, Fukushima Medical University, 1 Hikarigaoka, Fukushima 960-1295, Japan
e-mail: mgotoh@fmu.ac.jp

M. Terashima
Gastric Surgery Division, Shizuoka Cancer Center, Shizuoka, Japan

factor, is a reliable marker of Tregs [21–23], and immunostaining using specific antibody makes it possible to define Tregs more strictly as $CD4^+CD25^+Foxp3^+$ cells. Increased density of $Foxp3^+$ Tregs in cancer tissue has been seen in various cancers, including lung, liver, pancreas, ovary, and head and neck [24–28]. In a recent study, Mizukami et al. [29] reported that the localization pattern of Tregs was associated with clinical behavior in gastric cancer. The density of $Foxp3^+$ Tregs in relation to prognosis remain controversial, and there is a question whether infiltrating Tregs, in particular $Foxp3^+$ Tregs, are related to clinical outcome [30].

In this study, we focused on the density of $CD83^+$ DCs and $Foxp3^+$ Tregs in primary tumors and regional lymph nodes, from the viewpoint of two opposing factors in immune responses. We showed that the density of each cell type was inversely correlated with tumor progression and metastasis in the prognosis of patients with gastric cancer.

Patients, materials, and methods

Patients

We enrolled 123 patients (89 men, 34 women; age range 18–86 years, mean 66.9 years), who had undergone gastrectomy in the Fukushima Medical University Hospital between January 2000 and December 2004, and who had histologically proven gastric carcinoma. The follow-up period was from 2000 to 2009. Tumor characteristics were determined according to the *Japanese classification of gastric carcinoma* (JCGC) [31] and are listed in Table 1. The depth of tumor invasion (T category) and extent of lymph node metastasis (N category) were determined by histological diagnosis. There were 62 T1 tumors, 32 T2, 23 T3, and six T4. Lymph nodes were involved in 42 patients (N1 in 23, N2 in 12, and N3 in seven). Consequently, tumor stage was determined as IA in 55 patients, IB in 25, II in 10, IIIA in nine, IIIB in four, and IV in 20. Forty-two patients were lymph node-positive. The positive and negative lymph nodes were examined in 40 patients after excluding two that had all positive lymph nodes. In the 40 lymph-node-negative patients, regional lymph nodes were also examined. Patients with other malignant lesions upon preoperative clinical diagnosis were excluded from the examination. In addition, normal gastric tissue from 30 patients with early gastric cancer, taken far from the cancerous lesion in the same section, was used as a control.

Outcomes in patients with gastric cancer

Relapses occurred in 10 patients who had received curative surgery, because of the recurrence of peritoneal metastasis ($n = 6$), hepatic metastasis ($n = 3$), and lymph node metastasis ($n = 1$). Causes of death in the patients, including those with non-curative operations, were peritoneal metastasis ($n = 9$), hepatic metastasis ($n = 5$), and other diseases ($n = 10$). Patients who underwent non-curative surgery received postoperative chemotherapy using S-1, cisplatin, paclitaxel, or irinotecan, according to the choice of the physician.

Immunohistochemistry

Immunohistochemical reactions were performed using the streptavidin–biotin–peroxidase method. Anti-mouse CD83 monoclonal antibody (mAb) (clone HB15a; Santa Cruz Biotechnology, Heidelberg, Germany) and anti-mouse Foxp3 mAb (clone 236A/E7; Abcam, Cambridge, UK) were used. Tissue specimens including the deepest lesions of the primary tumor and lymph nodes were fixed in 10% neutral buffered formalin and embedded in paraffin. Sections were cut at 4-μm thicknesses, deparaffinized, and rehydrated. After the blocking of endogenous peroxidase with methanol containing 0.3% H_2O_2, for antigen retrieval, the sections were autoclaved at 121°C for 10 min in citrate buffer (10 mmol/l sodium citrate, pH 6.0) for staining with anti-Foxp3 mAb. The sections were boiled in a microwave oven for 15 min for staining with anti-CD83 mAb. After blocking with normal horse serum for Foxp3 or normal goat serum for CD83, the sections were reacted overnight with appropriately diluted primary antibodies. The sections were reacted sequentially with biotin-conjugated anti-mouse IgG antibodies (Vector Laboratories, Burlingame, CA, USA) and Vectastain Elite ABC reagent (Vector Laboratories). Immunohistochemical reactions were visualized with freshly prepared 3,3'-diamino-benzidine tetrahydrochloride. Slides were counterstained with hematoxylin and mounted on coverslips.

Quantification methods

Positively stained cells in normal gastric tissue, primary tumors, and lymph nodes were counted with a microscope (Nikon, Tokyo, Japan) at high power (400×) magnification. The tumor status of primary lesions and lymph nodes was determined by hematoxylin and eosin staining. We assessed each slide at the invasive margin of the tumor. We selected group 1 lymph nodes with and without metastasis classified by JCGC, and the normal gastric tissues in the patients with early gastric cancer were selected more than 1 cm away from carcinoma tissues. In each section, the degree of immune cell infiltration was observed in more than 10 independent high-power microscopic fields. The five areas with the most abundant distribution were selected without any previous knowledge of the patients'

Table 1 Patients' clinical characteristics

Clinicopathological factor[a]	No. of patients ($n = 123$)
Gender	
Male	89
Female	34
Age (years)	66.9 ± 11.4[b]
Range	18–86
Depth of tumor invasion	
T1	62
T2	32
T3	23
T4	6
Extent of lymph node metastasis	
N0	81
N1	23
N2	12
N3	7
Histological type	
Tubular (well/moderate)	67
Papillary	5
Poor	27
Signet	17
Mucinous	7
Histological stage	
IA	55
IB	25
II	10
IIIA	9
IIIB	4
IV	20

Well/moderate well-differentiated/moderately differentiated, *poor* poorly differentiated, *signet* signet ring cell

[a] Determined according to the *Japanese classification of gastric carcinoma* [31]

[b] Mean ± standard deviation

clinical backgrounds. We determined the total number of DCs and Foxp3$^+$ Tregs from five areas and then calculated the mean number for analysis of survival. Patients were divided into two groups for each variable, using median values as the cut-off points.

Statistical analysis

Statistical analysis was performed using StatView V.5.0 software (SAS Institute, Cary, NC, USA). Associations among the variables were assessed by the Mann–Whitney *U*-test and Kruskal–Wallis test. Survival curves were calculated using the Kaplan–Meier method and compared with the log-rank test. Both univariate and multivariate analyses of immune cell infiltration and clinicopathological features were performed using the Cox proportional hazards model. $P < 0.05$ was regarded as significant in all analyses.

Results

Immunohistochemical analysis of CD83$^+$ DCs and Foxp3$^+$ Tregs in gastric cancer tissues and lymph nodes

CD83$^+$ DCs and Foxp3$^+$ Tregs were specifically visualized immunohistochemically and quantified in normal gastric tissues, primary gastric cancers, and lymph nodes with or without metastasis (Fig. 1). The density of CD83$^+$ DCs decreased with cancer invasion; conversely, that of Foxp3$^+$ Tregs increased (Fig. 2a, b). CD83$^+$ DC infiltration in primary lesions was counted as 0–8 cells per high-power field (average 1.3), and Foxp3$^+$ Tregs as 0–64 (average 15.4). By contrast, CD83$^+$ DCs in normal gastric tissue were significantly higher in number than those in cancer tissue (average 3.4 vs. 1.3, $p < 0.0001$). The number of Foxp3$^+$ Tregs in primary lesions was significantly lower than that in normal tissue (average 15.4 vs. 2.2, $p < 0.0001$). The numbers of CD83$^+$ DCs and Foxp3$^+$ Tregs were inversely correlated. The number of CD83$^+$ DCs in positive lymph nodes was significantly lower than that in negative nodes in lymph node metastasis-negative [LNM(−)] cases, as well as in LNM(+) cases (average 1.1 vs. 3.5, 4.3, $p < 0.001$). Conversely, the number of Foxp3$^+$ Tregs in positive nodes was significantly higher than that in negative nodes in LNM(−) cases, as well as in LNM(+) cases (average 37.6 vs. 16.5, 18.3, $p < 0.001$). There was no significant difference between the number of CD83$^+$ DCs and Foxp3$^+$ Tregs in the negative lymph nodes of LNM(−) and LNM(+) cases.

Correlation between CD83$^+$ DCs, Foxp3$^+$ Tregs, and depth of tumor invasion

The density of CD83$^+$ DCs and and that of Foxp3$^+$ Tregs in the primary lesion were compared at different depths of tumor invasion (Fig. 2c, d). The average number of CD83$^+$ DCs in normal gastric tissue, and in T1, T2, T3, and T4 tumors was 3.4, 1.8, 1.3, 0.46, and 0.43, respectively. The corresponding number of Foxp3$^+$ Tregs was 2.2, 10.6, 22.9, 17.2, and 17.3, respectively. There was a significant difference between normal tissue and T1 tumors for the numbers of CD83$^+$ DCs and Foxp3$^+$ Tregs ($p < 0.0001$). A significant difference was also noted among T1, 2, 3, and 4 for CD83$^+$ DCs and Foxp3$^+$ Tregs ($p < 0.0001$).

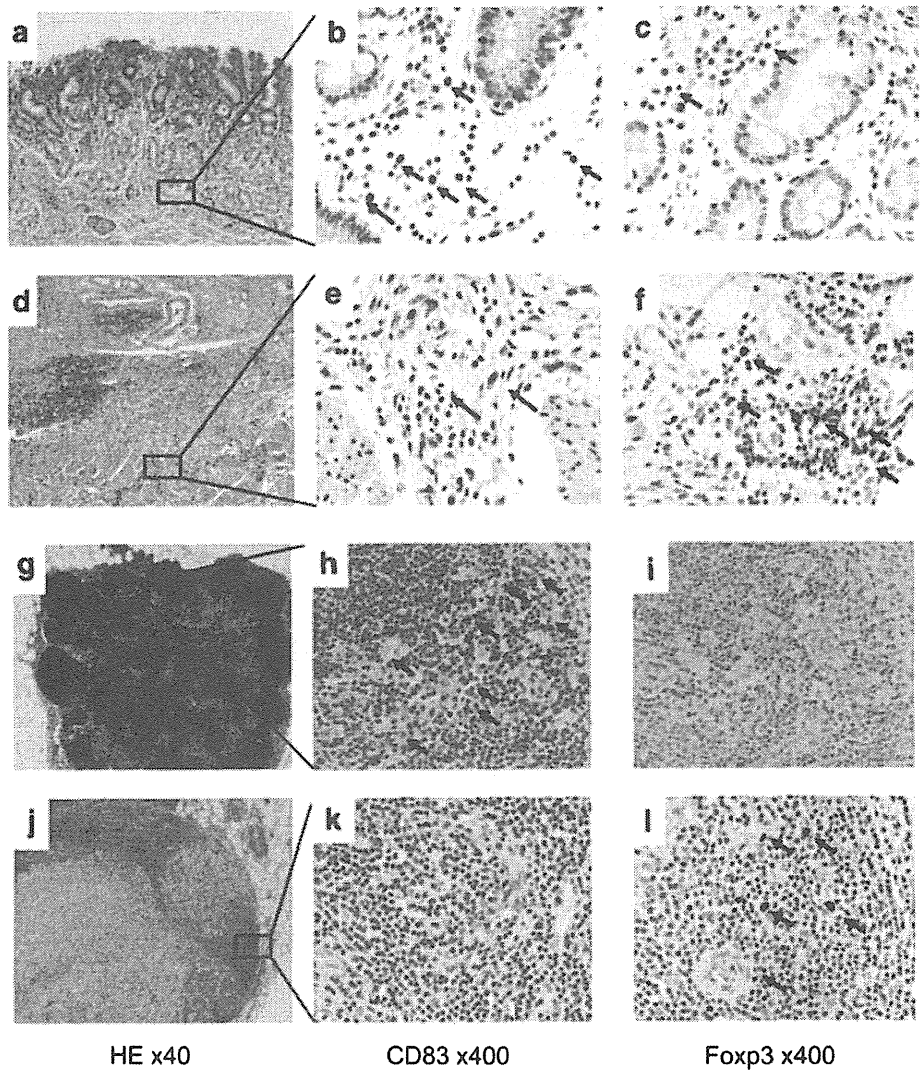

Fig. 1 Presence of $CD83^+$ and $Foxp3^+$ cells in gastric cancer. Immunohistochemical study of $CD83^+$ and $Foxp3^+$ cell recruitment was performed in normal gastric (**a–c**), cancerous (**d–f**), and negative (**g–i**) and positive (**j–l**) lymph node tissues. H&E stain (**a**, **d**, **g**, and **j**); $CD83^+$ cells (**b**, **e**, **h**, and **i**); and $Foxp3^+$ cells (**c**, **f**, **i**, and **l**). *Arrows* indicate positive cells. In normal gastric tissue, the density of $CD83^+$ cells was high (**b**) and that of $Foxp3^+$ cells was low (**c**). In contrast, in cancerous tissue, low dendritic cell (DC) infiltration (**e**) and a large population of $Foxp3^+$ cells (**f**) were observed. In negative lymph nodes, the density of $CD83^+$ cells was high (**h**) and that of $Foxp3^+$ cells was low (**i**). In contrast, in positive lymph nodes, these densities were inversely correlated (**k**, **i**)

Correlation between $CD83^+$ DCs, $Foxp3^+$ Tregs, and clinicopathological factors

The density of $CD83^+$ DCs and that of $Foxp3^+$ Tregs in primary lesions were examined in relation to clinicopathological status (Table 2). The numbers of $CD83^+$ DCs were significantly lower in patients with histologically undifferentiated-type tumors, positive LNM, hepatic metastasis, peritoneal invasion, positive peritoneal washing cytology, lymphatic vessel invasion, blood vessel invasion, greater depth of invasion, and higher histological stage. The numbers of $Foxp3^+$ Tregs were significantly higher in patients with positive LNM, peritoneal invasion, lymphatic vessel invasion, blood vessel invasion, greater depth of invasion, and higher histological stage, but there was no significant difference in numbers of $Foxp3^+$ Tregs in relation to histologically undifferentiated tumors, hepatic metastasis, and positive peritoneal washing cytology.

Univariate and multivariate analyses of survival in gastric cancer

We examined our results by univariate and multivariate analyses, using a Cox proportional hazards model. The clinicopathological factors listed in Table 2 were examined for their association with overall survival (OS) and disease-free survival (DFS) after initial surgery. In primary lesions, low numbers of $CD83^+$ DCs (Table 3a; OS: $p = 0.0122$, DFS: $p = 0.0016$) and high numbers of $Foxp3^+$ Tregs (OS: $p = 0.0222$, DFS: $p = 0.0250$) had a negative influence on OS and DFS in the univariate analysis. In negative lymph nodes in LNM(+) cases, low numbers of $CD83^+$ DCs also had a negative influence on OS and DFS in the univariate analysis (Table 3b; OS: $p = 0.0398$, DFS: $p = 0.0266$). In multivariate Cox proportional hazard analysis for clinicopathological variables, the high-$CD83^+$ DC group in primary lesions had a better prognosis than the low-$CD83^+$

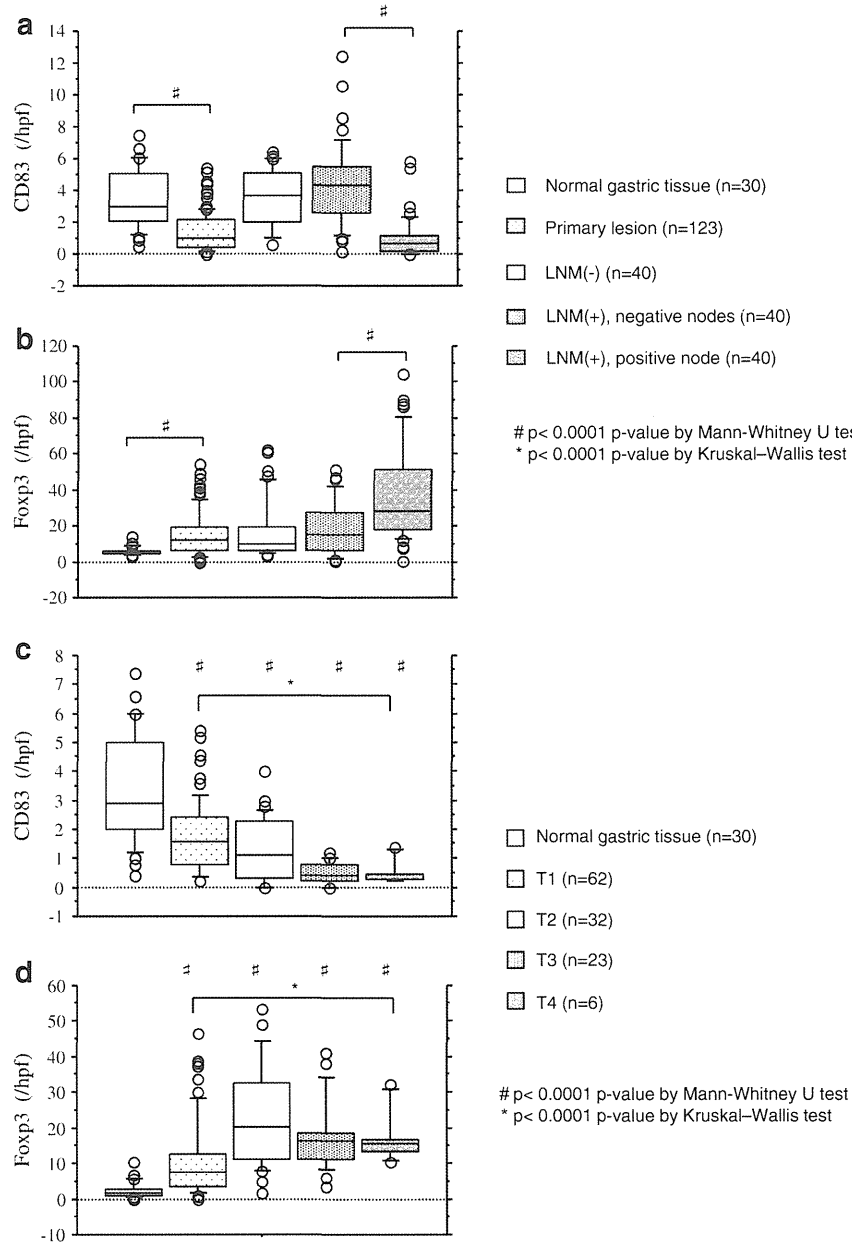

Fig. 2 Density of $CD83^+$ DCs and $Foxp3^+$ Tregs in gastric cancer and correlation of these densities with depth of cancer invasion. Numbers of $CD83^+$ DCs and $Foxp3^+$ regulatory T cells (Tregs) in primary lesions and lymph nodes (**a**, **b**) were examined and the number of these cells was examined in relation to the depth of tumor invasion (**c**, **d**). The density of $CD83^+$ DCs decreased with cancer invasion; conversely, that of $Foxp3^+$ Tregs increased in primary lesions, as well as in lymph nodes (**a**, **b**). The density of $CD83^+$ DCs and $Foxp3^+$ Tregs in primary lesions was inversely correlated with the depth of tumor invasion (**c**, **d**). #$p < 0.0001$ by Mann–Whitney test, *$p < 0.0001$ by Kruskal–Wallis test. *LNM* lymph node metastasis, *hpf* high-power field

DC group [Table 3a; OS: $p = 0.0374$, hazard ratio (HR) = 0.33, DFS: $p = 0.0118$, HR = 0.57]. The high number of $CD83^+$ DCs in negative lymph nodes in LNM(+) cases was identified as a significant prognostic predictor (Table 3b; OS: $p = 0.0296$, HR = 0.11, DFS: $p = 0.0078$, HR = 0.03).

Prognostic significance of $CD83^+$ DCs and $Foxp3^+$ Tregs in gastric cancer

We examined whether the presence of $CD83^+$ DCs and $Foxp3^+$ Tregs was correlated with prognosis, by Kaplan–Meier analysis. The high number of infiltrating $CD83^+$ DCs contributed greatly to both OS and DFS (Fig. 3a, b). The low-$Foxp3^+$ Tregs group showed significantly better OS than the high-$Foxp3^+$ Tregs group (Fig. 3c). The low-$Foxp3^+$ Tregs group also showed significantly better DFS than the high-$Foxp3^+$ Tregs group (Fig. 3d).

When the prognostic significance of $CD83^+$ DCs and $Foxp3^+$ Tregs was compared among four groups according to the respective parameters (CD83 low/high, Foxp3 low/high), the survival rate in patients with low-CD83/high-Foxp3 group was significantly poorer than that in the other three groups (Fig. 3e). This was also the case with the DFS (Fig. 3f). These results indicate that each cell type is inversely correlated with tumor progression and metastasis

Table 2 Correlation between CD83, Foxp3, and clinicopathological status

	All patients (n = 123)	CD83/hpf	p value	Foxp3/hpf	p value
Gender					
Male	89	1.52 ± 1.2		15.8 ± 12	
Female	34	1.27 ± 1.2	NS	14.3 ± 13	NS
Age (years)					
<60	27	1.05 ± 1.0		15.2 ± 11	
≧60	96	1.42 ± 1.2	NS	15.4 ± 13	NS
Histology					
Differentiated[a]	72	1.66 ± 1.3		14.2 ± 12	
Undifferentiated[b]	51	0.88 ± 0.9	0.0003	17.1 ± 12	NS
Lymph node metastasis					
Negative	81	1.75 ± 1.2		14.2 ± 13	
Positive	42	0.55 ± 0.6	<0.0001	17.7 ± 10	0.0063
Hepatic metastasis					
Absent	116	1.40 ± 1.2		15.3 ± 12	
Positive	7	0.31 ± 0.4	0.0041	16.1 ± 8.9	NS
Peritoneal invasion					
Absent	112	1.43 ± 1.2		14.9 ± 12	
Positive	11	0.35 ± 0.3	0.0007	20.4 ± 9.6	0.0377
Cytology in peritoneal washings					
Negative	115	1.40 ± 1.2		15.2 ± 13	
Positive	8	0.48 ± 0.43	0.0196	18.1 ± 6.2	NS
Lymphatic vessel invasion					
Negative	47	1.94 ± 1.3		11.3 ± 12	
Positive	76	0.97 ± 0.9	<0.0001	17.9 ± 12	<0.0001
Blood vessel invasion					
Negative	54	1.70 ± 1.2		10.9 ± 10	
Positive	69	1.06 ± 1.1	0.0005	18.9 ± 12	<0.0001
Depth of invasion					
T1	62	1.77 ± 1.2		10.7 ± 11	
T2–4	61	0.90 ± 0.9	<0.0001	20.2 ± 12	<0.0001
Histological stage					
I, II	90	1.68 ± 1.2		14.4 ± 13	
III, IV	33	0.39 ± 0.4	<0.0001	18.0 ± 8.7	0.0083

Data are means ± SD

p value by Mann–Whitney U-test

NS not significant, *hpf* high-power field

[a] Differentiated; papillary or tubular adenocarcinoma

[b] Poorly differentiated or undifferentiated adenocarcinoma, signet-ring-cell carcinoma, or mucinous adenocarcinoma

in the prognosis of patients with gastric cancer. When the prognostic significance of $CD83^+$ DCs and $Foxp3^+$ Tregs in negative lymph nodes in gastric cancer with LNM was examined, the density of CD83 in non-metastatic lymph nodes was found to be associated with prognosis (Fig. 4). The high number of infiltrating DCs contributed greatly to both OS and DFS.

Discussion

Two opposing components of immune responses were examined in primary gastric cancer and regional lymph nodes. $CD83^+$ DCs were decreased in proportion to the stage of cancer (i.e., the lower the $CD83^+$ DC density, the higher the stage), and a low density was significantly

Table 3 Univariate and multivariate analyses of prognostic factors associated with OS and DFS

Prognostic factors	OS			DFS		
	Univariate (*p*)	Multivariate (*p*)	HR (95% CI)	Univariate (*p*)	Multivariate (*p*)	HR (95% CI)
(a) All cases						
Gender (male or female)	0.4294			0.4400		
Age (<60 years)	0.5539			0.4727		
Lymphatic vessel invasion	0.0864			0.0206	0.2768	0.27 (0.03–2.87)
Blood vessel invasion	0.1453			0.0212	0.7457	0.75 (0.13–4.34)
Histology (differentiated or undifferentiated)	0.0826			0.0007	0.0296	0.21 (0.05–0.86)
Cytology	<0.0001	<0.0001	0.57 (0.02–0.20	0.0015	0.1547	0.37 (0.09–1.46)
Hepatic metastasis	0.0424	0.6020	0.60 (0.17–2.20)	0.0039	0.6116	0.72 (0.19–2.57)
pT1 vs. pT2-4	0.0420	1.1940	1.19 (0.27–5.34)	0.0029	0.0350	0.04 (0.002–0.80)
CD83 (high or low)	0.0122	0.0374	0.33 (0.12–0.95)	0.0016	0.0118	0.57 (0.006–0.54)
Foxp3 (high or low)	0.0222	0.2257	2.10 (0.63–6.93	0.0250	0.5234	0.64 (0.16–2.51)
(b) LNM (+) cases						
Gender (male/female)	0.4864			0.2839		
Age (<60 years)	0.3428	0.0335	12.59 (1.22–130.01)	0.8877		
Lymphatic vessel invasion	–			–		
Blood vessel invasion	0.7588			0.8847		
Histology (differentiated or undifferentiated)	0.5693			0.0476	0.0059	0.004 (0.001–0.20)
Cytology	0.0049	0.0019	0.01 (0.001–0.20)	0.4475		
Hepatic metastasis	0.5693			0.4755		
pT1 vs. pT2-4	0.4472			–		
CD83 LNM (+), node-positive	0.2356			0.2093		
CD83 LNM (+), node-negative	0.0398	0.0296	0.11 (0.01–0.80)	0.0266	0.0078	0.03 (0.002–0.39)
Foxp3 LNM (+), node-positive	0.8072			0.4657		
Foxp3 LNM (+), node-negative	0.5308			0.4121		

OS overall survival, *DFS* disease-free survival, *HR* hazard ratio, *CI* confidence interval, *LNM* lymph node metastasis

correlated with poor prognosis. Conversely, $Foxp3^+$ Tregs were increased in proportion to the stage of cancer (i.e., the higher the $Foxp3^+$ Tregs density, the higher the stage), and a high density was significantly correlated with poor prognosis. The density of $CD83^+$ DCs and $Foxp3^+$ Tregs in metastatic lymph nodes was similar to that in primary lesions, when compared with that in negative lymph nodes. This is, to the best of our knowledge, the first study to show that two opposing factors in the immune response in primary lesions, as well as in metastatic lymph nodes, were inversely related.

Immature DCs with a protein S100 marker, as well as mature DCs with a CD83 marker, have been shown to be correlated with the prognosis of various cancers [32–36]. Tsujitani et al. [32] have reported that infiltrating S100-positive DCs do not prevent the spread of tumor invasion but do prevent nodal involvement. In the present study, the high number of infiltrating DCs contributed to both OS and DFS in negative lymph nodes in gastric cancer with LNM. Tumor-infiltrating DCs exhibit various phenotypes and functions depending on their maturation status. The expression of S100 on DCs is not specific; therefore, we evaluated maturation-specific tissue infiltration of DCs. We found that the density of CD83 + DCs was significantly decreased in T1 tumors (tumor invasion within the submucosal layer), and it decreased further in relation to tumor progression. The density of CD83 in primary lesions was a highly independent prognostic factor by both univariate and multivariate analyses. These data were consistent with earlier studies.

The density of $Foxp3^+$ Tregs in gastric cancer was significantly correlated with prognosis in the present study. A significant increase in the density of these cells was found in T1 tumors, and the density of these cells was further increased in relation to tumor progression. Mizukami et al. [29] have reported that the pattern of localization of $Foxp3^+$ Tregs, rather than the population of these cells counted in randomly selected areas, is associated with

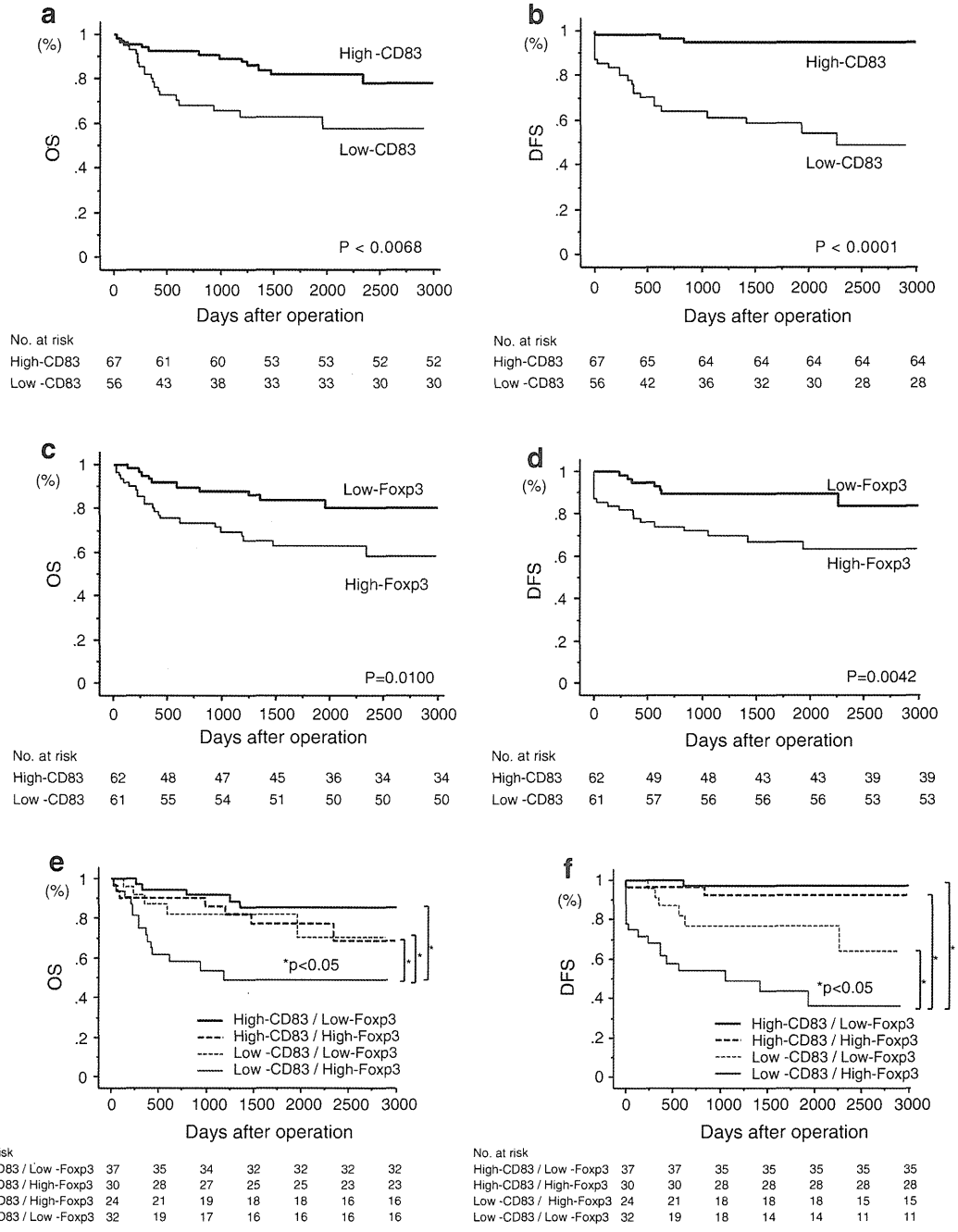

Fig. 3 Prognostic significance of $CD83^+$ DCs and $Foxp3^+$ Tregs in gastric cancer. The density of $CD83^+$ DCs and $Foxp3^+$ Tregs in primary lesions was examined in relation to prognosis by Kaplan–Meier analysis (**a–f**). A high $CD83^+$ DC level contributed to both overall survival (*OS*) (**a**) and disease-free survival (*DFS*) (**b**). A low $Foxp3^+$ Tregs level contributed to OS (**c**) and DFS (**d**). The density of $CD83^+$ DCs and $Foxp3^+$ Tregs in primary lesions was divided into four groups: high-CD83/low-Foxp3 ($n = 37$), high-CD83/high-Foxp3 ($n = 30$), low-CD83/low-Foxp3 ($n = 24$), and low-CD83/high-Foxp3 group ($n = 32$). OS and DFS in patients with the low-CD83/high-Foxp3 group were significantly shorter compared with those for the other three groups (**e**, **f**). *p* value was determined by log-rank test

clinical behavior in gastric cancer. We examined the degree of immune cell infiltration at the deepest area of tumor invasion. Our study had more stage I patients compared with that of Mizukami et al. (62/123 vs. 31/80). The difference in these factors might explain the difference in results, but needs to be evaluated in a prospective study.

The density of $CD83^+$ DCs is particularly interesting because antigen-pulsed DCs migrate to lymph nodes, in which

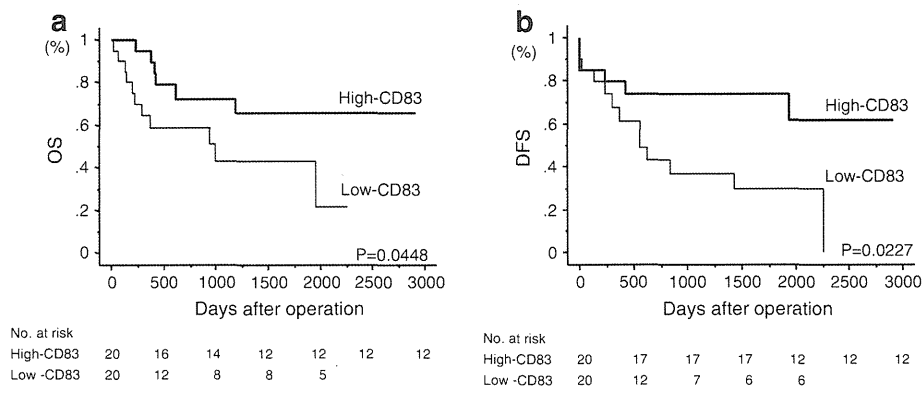

Fig. 4 Prognostic significance of $CD83^+$ DCs in lymph nodes of gastric cancer. The density of $CD83^+$ DCs in negative nodes of metastasis-positive cases was examined in relation to the prognosis of these patients. A high $CD83^+$ DC level in the negative nodes of metastasis-positive cases contributed to both OS (**a**) and DFS (**b**). *p* value was determined by log-rank test

they activate certain types of T cells, which leads to cytotoxic T-lymphocyte generation. However, no data were available for $CD83^+$ DCs or $Foxp3^+$ Tregs in the regional lymph nodes of gastrointestinal cancer. We found that the density of $CD83^+$ DCs and $Foxp3^+$ Tregs in lymph nodes was similar to that in primary tumors. Thus, with metastasis, the density of $CD83^+$ DCs decreased and, conversely, that of $Foxp3^+$ Tregs increased. This is consistent with the previous findings of Kawaida et al. [37], who have shown that the numbers of $CD4^+CD25^{high}$ Tregs in the regional lymph nodes in patients with gastric cancer are significantly higher than those in control lymph nodes. In the present study, it was interesting that the density of $CD83^+$ DCs in negative lymph nodes in patients with lymph node metastasis was found to be an independent prognostic factor. Although the density of $CD83^+$ DCs in negative lymph nodes in patients with LNM was slightly higher than that in the negative lymph nodes of patients without metastasis, the density of $CD83^+$ DCs in lymph nodes may be an independent prognostic factor in patients with LNM. A low density of $CD83^+$ DCs was correlated with poor prognosis and shorter DFS. This might have resulted from a decreased systemic response in the patients or the possibility of micro-metastasis in the lymph nodes. This is believed to be the first study to show a correlation between the immune response in lymph nodes and the prognosis of gastric cancer. However, further clarification of this correlation, as well as the concept of sentinel lymph nodes, is needed in future studies.

DC maturation is a continuous process that is initiated in the periphery upon antigen encounter and/or by inflammatory cytokines, and is completed during DC–T cell interaction. Numerous factors induce and/or regulate DC maturation, including pathogen-related molecules such as lipopolysaccharide, bacterial DNA, and the balance between pro- and anti-inflammatory signals in the local microenvironment, including tumor necrosis factor, interleukin (IL)-1, IL-6, IL-10, and transforming growth factor (TGF)-β [1]. Cancer cells are known to produce certain cytokines such as IL-6, IL-10, TGF-β, and vascular endothelial growth factor, which do suppress DC maturation. $CD4^+CD25^{high}$ $Foxp3^+$ T cells also secrete IL-10 and TGF-β, which both mediate suppression of immune responses in the tumor microenvironment [38]. Recently, Sarrs et al. [39] have found that neuropilin-1, which is expressed by most Tregs, but not naïve T-helper cells, promotes prolonged interaction with immature DCs, which suggests the default suppression of immune responses in the absence of danger signals. Terme et al. [40] have also reported that Tregs control DC/NK cell crosstalk in lymph nodes in the steady state by inhibiting $CD4^+$ self-reactive T cells. In line with these data, it is reasonable to assume that a high density of $Foxp3^+$ Tregs plays an important role, directly or indirectly, in inhibiting the local activation of DCs.

We elucidated two arms of the immune response to cancer: immunoactivation and immunosuppression. For these immune responses, $CD83^+$ DCs and $Foxp3^+$ Tregs were investigated in primary lesions and regional lymph nodes. Similar trends were found at both sites in association with tumor invasion. For cell-targeted immunotherapy, DCs can be injected directly into the tumor. The elimination of Tregs has been trialed in basic [41, 42] and clinical [43] settings, with some promising results [44]. To further investigate the efficacy of the elimination of Tregs, careful monitoring of the two arms of the immune response will be needed.

References

1. Banchereau J, Briere F, Caux C, et al. Immunobiology of dendritic cells. Annu Rev Immunol. 2000;18:767–811.
2. Zhou LJ, Schwarting R, Smith HM, Tedder TF. A novel cell-surface molecule expressed by human interdigitating reticulum cells, Langerhans cells, and activated lymphocytes is a new member of the Ig superfamily. J Immunol. 1992;149:735–42.
3. Zhou LJ, Tedder TF. Human blood dendritic cells selectively express CD83, a member of the immunoglobulin superfamily. J Immunol. 1995;154:3821–35.
4. Bell D, Chomarat P, Broyles D, et al. In breast carcinoma tissue, immature dendritic cells are located in peritumoral areas. J Exp Med. 1999;190:1417–25.

5. Zhou L, Tedder TF. $CD14^+$ blood monocytes can differentiate into functionally mature $CD83^+$ dendritic cells. Immunology. 1999;93:2588–92.
6. Thurner M, Radmayr C, Ramoner R, et al. Human renal-cell carcinoma tissue contain dendritic cells. Int J Cancer. 1996;68:1–7.
7. Tsukayama S, Omura K, Yoshida K, Tanaka Y, Watanabe G. Prognostic value of CD83 positive mature dendritic cells and their relation to vascular endothelial growth factor in advanced human gastric cancer. Oncol Rep. 2005;14:369–75.
8. Saito H, Osaki T, Murakami D, et al. Prediction of sites of recurrence in gastric carcinoma using immunohistochemical parameters. J Surg Oncol. 2007;95:123–8.
9. Naito Y, Saito K, Shibata K, et al. $CD8^+$ T cells infiltrated within cancer cell nests as a prognostic factor in human colorectal cancer. Cancer Res. 1998;58:3491–4.
10. Furihata M, Ono Y, Ichikawa K, Tomita S, Fujimori T, Kubota K. Prognostic significance of CD83 positive, mature dendritic cells in the gallbladder carcinoma. Oncol Rep. 2005;14:353–6.
11. Miyagawa S, Soeda J, Takagi S, Miwa S, Ichikawa E, Noike T. Prognostic significance of mature dendritic cells and factors associated with their accumulation in metastatic liver tumors from colorectal cancer. Hum Pathol. 2004;35:1392–6.
12. Iwamoto M, Shinohara H, Miyamoto A, et al. Prognostic value of tumor-infiltrating dendritic cells expressing CD83 in human breast carcinomas. Int J Cancer. 2003;104:92–7.
13. Jonuleit H, Schmitt E, Stassen M, Tuettenberg A, Knop J. Identification and functional characterization of human $CD4^+CD25^+$ T cells with regulatory properties isolated from peripheral blood. J Exp Med. 2001;193:1285–94.
14. Ng WF, Duggan PJ, Ponchel F, et al. Human $CD4^+CD25^+$ cells: a naturally occurring population of regulatory T cells. Blood. 2001;98:2736–44.
15. Sakaguchi S, Sakaguchi N, Asano M, Itoh M, Toda M. Immunologic self-tolerance maintained by activated T cells expressing IL-2 receptor α-chains (CD25). J Immunol. 1995;155:1151–64.
16. Sakaguchi S, Ono M, Setoguchi R, et al. $Foxp3^+CD25^+CD4^+$ natural regulatory T cells in dominant self-tolerance and autoimmune disease. Immunol Rev. 2006;212:8–27.
17. Dejaco C, Dultner C, Grubeck B, Schirmer M. Imbalance of regulatory T cells in human autoimmune diseases. Immunology. 2005;117:289–300.
18. Beyer M, Schulze JL. Regulatory T cells in cancer. Blood. 2006;108:804–11.
19. Viehl C, Moore T, Liyanaga U, et al. Depletion of $CD4^+CD25^+$ regulatory T cells promotes a tumor-specific immune response in pancreas cancer-bearing mice. Ann Surg Oncol. 2005;13:1252–8.
20. Rudge G, Barrett SP, Scott B, Driel IR. Infiltration of a mesothelioma by IFN-γ-producing cells and tumor rejection after depletion of regulatory T cells. J Immunol. 2007;178:4089–96.
21. Hori S, Nomura T, Sakaguchi S. Control of regulatory T cells development by the transcription factor Foxp3. Science. 2003;299:1057–61.
22. Fontenot JD, Gavin MA, Rudensky A. Foxp3 programs the development and function of $CD4^+CD25^+$ regulatory T cells. Nat Immunol. 2003;10:1330–6.
23. Fontenot JD, Rasmussen JP, Williams M, Dooley L, Farr AG, Rudensky Y, et al. Regulatory T cell lineage specification by the forkhead transcription factor foxp3. Immunity. 2005;22:329–41.
24. Woo EY, Chu CS, Goletz TJ, et al. Regulatory $CD4^+CD25^+$T cells in tumors from patients with early-stage non-small cell lung cancer and last-stage ovarian cancer. Cancer Res. 2001;61:4766–72.
25. Badoual C, Hans S, Rodriguez J, et al. Prognostic value of tumor-infiltrating C^+ T cells subpopulations in head and neck cancers. Clin Cancer Res. 2006;12:465–72.
26. Wolf D, Wolf A, Rumpold H, et al. The expression of the regulatory T cell-specific forkhead box transcription factor FoxP3 is associated with poor prognosis in ovarian cancer. Clin Cancer Res. 2005;11:8326–31.
27. Kobayashi N, Hiraoka N, Yamagami W, et al. $FOXP3^+$ regulatory T cells affect the development and progression of hepatocarcinogenesis. Clin Cancer Res. 2007;13:902–11.
28. Hiraoka N, Onozato K, Kosuge T, Hirohashi S. Prevalence of $FOXP3^+$ regulatory T cells increases during the progression of pancreatic ductal adenocarcinoma and its premalignant lesions. Clin Cancer Res. 2006;12:5423–34.
29. Mizukami Y, Kono K, Kawaguchi Y, et al. Localisation pattern of $Foxp3^+$ regulatory T cells is associated with clinical behaviour in gastric cancer. Br J Cancer. 2008;98:148–53.
30. Siddiqui SA, Frigola X, Bonne-Annee S, et al. Tumor-infiltrating $Foxp3\text{-}CD4^+CD25^+$ T cells predict poor survival in renal cell carcinoma. Clin Cancer Res. 2007;13:2075–81.
31. Japanese Gastric Cancer Association. Japanese classification of gastric carcinoma, 2nd English edition. Gastric Cancer. 1998;1:10–24.
32. Tsujitani S, Kakeji Y, Watanabe A, Kohnoe S, Maehara Y, Sugimachi K. Infiltration of dendritic cells in relation to tumor invasion and lymph node metastasis in human gastric cancer. Cancer. 1990;66:2012–6.
33. Dadabayev A, Sandel M, Menon A, et al. Dendritic cells in colorectal cancer correlate with other tumor-infiltrating immune cells. Cancer Immunol Immunother. 2004;53:978–86.
34. Miyake M, Taki T, Hitomi S, Hakomori S. Correlation of expression of H/Ley/Leb antigen with survival in patients with carcinoma of the lung. N Engl J Med. 1992;327:14–8.
35. Matsuda H, Mori M, Tsujitani S, Ohno S, Kuwano H, Sugimachi K. Immunohistochemical evaluation of squamous cell carcinoma antigen and S-100 protein-positive cells in human malignant esophageal tissues. Cancer. 1990;65:2261–5.
36. Schwaab T, Weiss JE, Schned AR, Barth RJ Jr. Dendritic cell infiltration in colon cancer. J Immunother. 2001;24:130–7.
37. Kawaida H, Kono K, Takahashi A, et al. Distribution of CD4(+)CD25 high regulatory T-cells in tumor-draining lymph nodes in patients with gastric cancer. J Surg Oncol. 2005;124:151–7.
38. Strauss L, Bergmann C, Szczepanski M, Gooding W, Johnson JT, Whiteside TL. A unique subset of $CD4^+CD25highFoxp3^+$ T cells secreting interleukin-10 and transforming growth factor-beta1 mediates suppression in the tumor microenvironment. Clin Cancer Res. 2007;13:4345–54.
39. Sarrs M, Andersen KG, Randow F, Mayr L, Betz AG. Neuropilin-1 expression on regulatory T cells enhances their interactions with dendritic cells during antigen recognition. Immunity. 2008;28:402–13.
40. Terme M, Chaput N, Combadiere B, Ma A, Ohteki T, Zitvogel L. Regulatory T cells control dendritic cell/NK cell cross-talk in lymph nodes at the steady state by inhibiting $CD4^+$ self-reactive T cells. J Immunol. 2008;180:4679–86.
41. Fehervari A, Sakaguchi S. Control of $Foxp3^+CD4^+$ regulatory cell activation and function by dendritic cells. Int Immunol. 2004;16:1769–80.
42. Yamaguchi T, Hirota K, Nagahama K, et al. Control of immune responses by antigen-specific regulatory T cells expressing the folate receptor. Immunity. 2007;27:145–59.
43. Schmidt J, Eisold S, Büchler MW, Märten A. Dendritic cells reduce number and function of $CD4^+CD25^+$ cells in cytokine-induced killer cells derived from patients with pancreatic carcinoma. Cancer Immunol Immunother. 2004;53:1018–26.
44. Van Meirvenne S, Dullaers M, Heirman C, Straetman L, Michiels A, Thielemans K. In vivo depletion of $CD4^+CD25^+$ regulatory T cells enhances the antigen-specific primary and memory CTL response elicited by mature mRNA-electroporated dendritic cells. Mol Ther. 2005;12:922–32.

Original Paper

Digestive Surgery

Dig Surg 2012;29:115–123
DOI: 10.1159/000336949

Received: September 7, 2011
Accepted after revision: January 28, 2012
Published online: March 27, 2012

Activation of the Sonic Hedgehog Pathway and Its Prognostic Impact in Patients with Gastric Cancer

Zenichiro Saze[a] Masanori Terashima[b] Michihiko Kogure[a] Fumihiko Ohsuka[a]
Hiroyuki Suzuki[a] Mitsukazu Gotoh[a]

[a]First Department of Surgery, Fukushima Medical University, Fukushima, and [b]Gastric Surgery Division, Shizuoka Cancer Center, Shizuoka, Japan

Key Words
Sonic hedgehog pathway · Gastric cancer · Prognosis

Abstract
Background: The sonic hedgehog (SHH) signaling pathway is critical in fetal organogenesis. Activation of the SHH pathway has been associated with several types of human cancer; however, the clinical impact of SHH activation in patients with gastric cancer is still unknown. ***Methods:*** The present study included 41 patients with gastric cancer who underwent gastrectomy between 2000 and 2004. SHH, Patched-1 (PTCH1), Smoothened (SMO) and Glioma-associated oncogene-1 (GLI1) were examined immunohistochemically, and these of mRNAs from the cancer lesions were evaluated using real-time quantitative RT-PCR. ***Results:*** Immunohistological expressions of SHH-related molecules were relatively intense in cancer tissue, but no significant correlation was found with any clinicopathological factors of tumor. PTCH1 was only the molecule associated with poor prognosis of patients with differentiated type of tumor. For mRNA analysis, a significant correlation was demonstrated between certain clinicopathological factors and *PTCH1*, *SMO* or/and *GLI1* mRNA levels. High levels of *SHH* and *PTCH1* mRNA were associated with poor prognosis. Multivariate analysis demonstrated the *PTCH1* mRNA level and liver metastasis as significant independent prognostic factors. ***Conclusions:*** *PTCH1* expression in the SHH pathway was possibly involved in gastric cancer tumor progression, and could be a useful indicator for the prognosis of gastric cancer.

Introduction

The Sonic hedgehog (SHH) signaling pathway plays an important role in human embryonic development [1, 2]. SHH signaling is mediated via a series of inhibitory steps [1]. After secretion, the diffusion of SHH ligand is limited by binding to the Patched-1 (PTCH1) transmembrane receptor. In the absence of ligand, PTCH1 receptors block the function of another transmembrane protein, Smoothened (SMO), and this inhibition is relieved following ligand binding. As a consequence, SMO becomes active and initiates a signaling cascade that results in the activation of the Glioma-associated oncogene-1 (GLI1) transcription factor. In the absence of ligands, GLI1 is linked to the cytoskeleton via interaction with a multiprotein complex that includes Fused (FU) and Suppressor of fused (SUFU). Following ligand binding, GLI1 translocates into the nucleus where it controls the transcription of target genes. Thus, SHH signaling is regulated at nu-

KARGER
Fax +41 61 306 12 34
E-Mail karger@karger.ch
www.karger.com

0253–4886/12/0292–0115$38.00/0

Accessible online at:
www.karger.com/dsu

Mitsukazu Gotoh, MD
First Department of Surgery, Fukushima Medical University
1 Hikarigaoka
Fukushima 960-1295 (Japan)
Tel. +81 24 547 1252, E-Mail mgotoh@fmu.ac.jp

merous levels by different components of the pathway; a peculiar phenomenon, which suggests that tight control of SHH activity is crucial for its proper function [1].

Activation of SHH signaling, through loss-of-function mutations of PTCH1 or activation mutations of SMO, occurs frequently in human basal cell carcinoma (BCC) and medulloblastoma [3–7]. More recently, abnormal activation of the SHH pathway has been reported in small cell lung cancer, pancreatic cancer, prostate cancer, and gastrointestinal cancers [8–14]. In gastric cancers, activation of the SHH pathway has been described [15–18], but correlation of SHH pathway activation with prognosis remains to be determined.

In this study, we used real-time quantitative RT-PCR (RQ-PCR) to assay SHH pathway molecules to investigate correlations between the activation of the SHH pathway and clinicopathological factors. We also correlated expression of pathway molecules with the prognosis of patients with gastric cancer.

Materials and Methods

Tissue Samples

Gastric cancer tissues were obtained from 41 patients who underwent gastrectomy at Fukushima Medical University between January 2000 and December 2004 after approval from the medical ethics committee and acquisition of informed consent. Patient characteristics were determined according to the Japanese Classification of Gastric Carcinoma (2nd English edition; table 1). Cancers tissues were histologically classified as: (a) differentiated-type adenocarcinoma, including papillary adenocarcinoma and tubular adenocarcinoma, and (b) undifferentiated-type adenocarcinoma, including poorly differentiated adenocarcinoma, mucinous adenocarcinoma and signet ring cell carcinoma. Normal epithelial tissues were obtained from the resected specimen as far as possible from the cancer lesion (n = 9), and were used as control.

Immunohistochemistry

Resected specimens were fixed with 10% buffered formalin and embedded in paraffin. Tissue blocks were then sliced into 4-μm sections and mounted on glass slides. The sections were pretreated in 10 mM citrate buffer (pH 6) by a microwave-based antigen retrieval method for 15 min and then incubated with monoclonal anti-human SHH, PTCH1, SMO and GLI1 antibody (Santa Cruz Biotechnology Inc., Calif., USA) at a dilution of 1:100 overnight. Histofine SAB-PO kit (Nichirei, Tokyo, Japan) was used to visualize antibody binding. Immnoreactivity of those proteins was classified into two types: focal (<50%) and diffuse (≥50%) by expression ratio.

RNA Extraction and cDNA Synthesis

RNA was extracted using an RNeasy Mini Kit™ and QIA shredder™ (Qiagen GmbH, Hilden, Germany). Total RNA (1 μg) was reverse-transcribed using random hexamer, SuperScript II reverse transcriptase™ (Invitrogen, Carlsbad, Calif., USA) and 10 M dNTPs (Sigma-Aldrich, St. Louis, Mo., USA). Reverse transcriptase-polymerase chain reaction (RT-PCR) was performed using the Gene Amp PCR System™ (Applied Biosystems, Foster City, Calif., USA). Integrity of the isolated RNA was established by RT-PCR analysis of the housekeeping gene, glyceraldehyde-3-phosphate dehydrogenase *(GAPDH).*

Table 1. Patient characteristics

Gender	
Male	30
Female	11
Age, years	30–86 (mean 64.8)
Histological type	
pap	1
tub1	6
tub2	9
por1	4
por2	8
sig	7
muc	4
small	2
Depth of invasion	
T1	5
T2	13
T3	17
T4	6
Stroma in tumors	
Sci	13
Int	19
Med	9
Lymph node metastasis	
N0	11
N1	14
N2	10
N3	6
Peritoneal metastasis	
P0	35
P1	6
Hepatic metastasis	
H0	37
H1	4
Stage	
IA	3
IB	7
II	4
IIIA	7
IIIB	5
IV	15

pap = Papillary adenocarcinoma; tub1 = well-differentiated tubular adenocarcinoma; tub2 = moderately-differentiated tubular adenocarcinoma; por1 = poorly differentiated adenocarcinoma (solid type); por2 = poorly differentiated adenocarcinoma (non-solid type); sig = signet ring cell carcinoma; muc = mucinous adenocarcinoma; Sci = scirrhous type; Int = intermediate type; Med = medullary type.

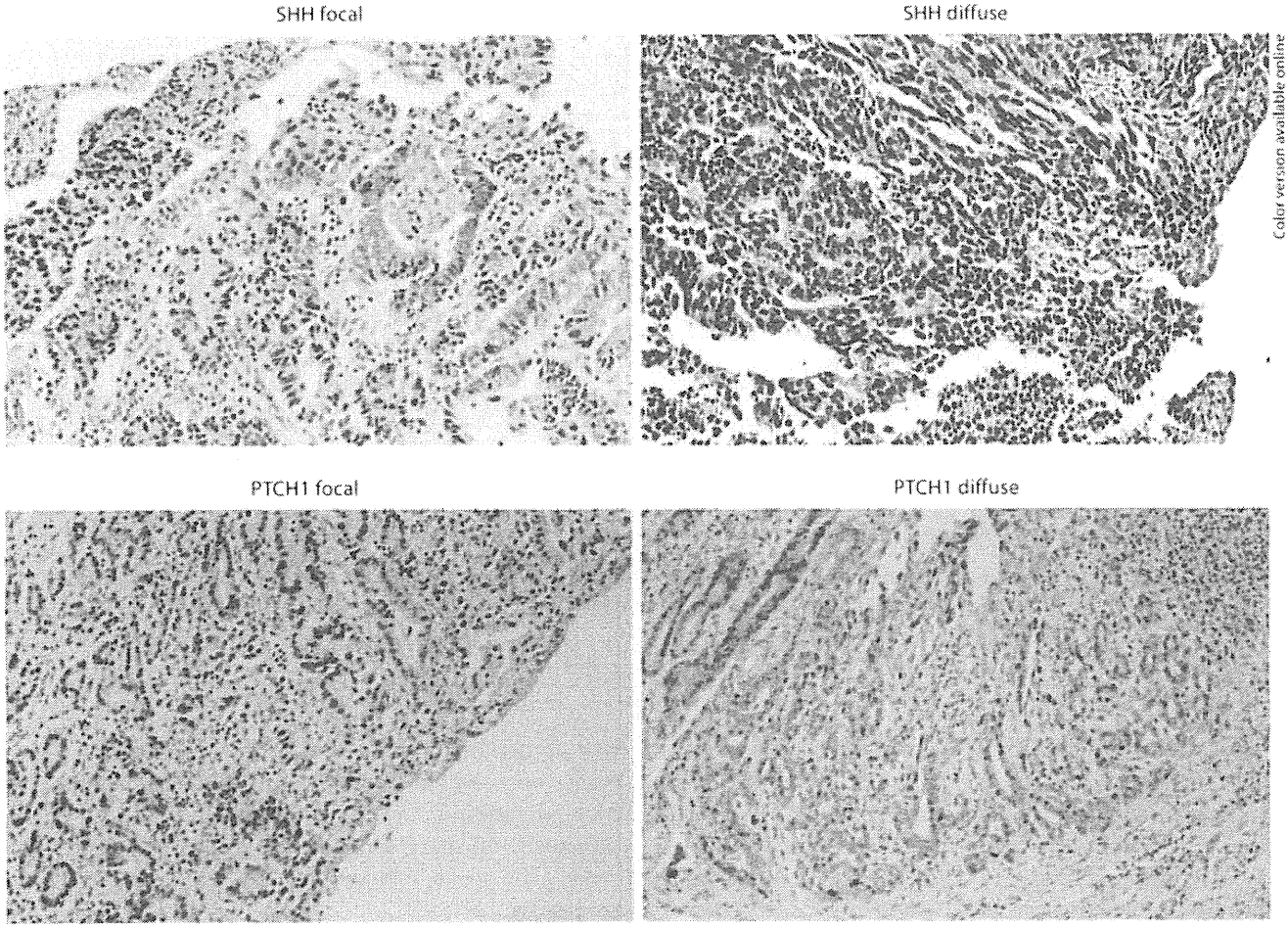

Fig. 1. Immunoreactivity of SHH and PTCH1 in cancer tissue. Patients were divided into focal and diffuse expression groups according to positive area ratio in cancer tissue.

Real-Time Quantitative Polymerase Chain Reaction

RQ-PCR was performed using an ABI Prism 7000 Sequence Detection System™ (Applied Biosystems). PCR reactions (50 μl) contained 2.5 μl of TaqMan gene expression assay™ solution (Applied Biosystems), including *SHH*, *PTCH1*, *SMO* and *GLI1* specific oligonucleotide primers (assay ID Hs00179843_m1, Hs00181117_m1, Hs00170665_m1 and Hs00171790_m1), 25 μl of TaqMan Universal PCR Master Mix™ (Applied Biosystems), and 2 μl of cDNA sample. Amplification was performed for 50 cycles at 95°C for 15 s and 60°C for 1 min. mRNA levels were normalized against *GAPDH* mRNA levels.

Statistical Analysis

Statistical analyses were performed using SPSS 17 for Windows (SPSS, Chicago, Ill., USA). The Mann-Whitney test for independence was used to determine the strength of correlations between *SHH*, *PTCH1*, *SMO* and *GLI1* expression and clinicopathological factors. The Pearson's correlation coefficient was used to determine the strength of correlation between the expression of each molecule in the SHH pathway.

Survival time was estimated using the Kaplan-Meier method, and the log-rank test was used for testing differences in survival time between groups. The multivariate Cox proportional hazard model was applied to detect independent predictors of survival. Values of $p < 0.05$ were considered statistically significant.

Results

Immunoreactivity of Cancer Tissue and Normal Epithelium

There were no significant correlation between SHH, PTCH1, SMO and GLI1 expression and clinicopathological factors by immunohistochemical analysis (data not

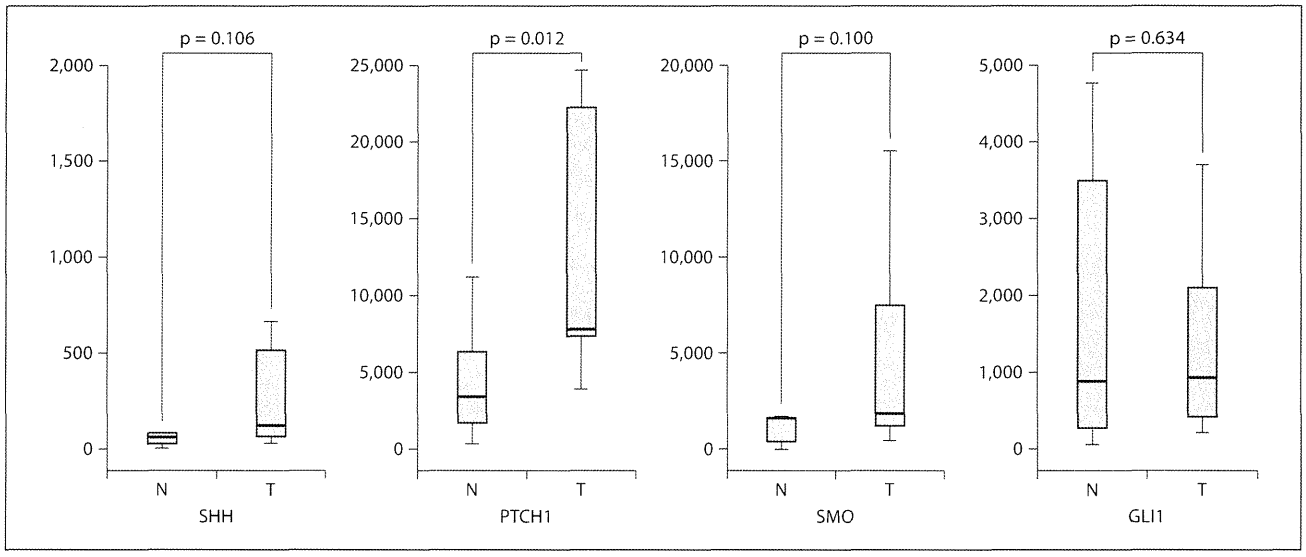

Fig. 2. Comparison between the expression of SHH pathway-associated molecules in tumor tissues and normal epithelium. *PTCH1* mRNA levels were significantly higher in cancer tissue compared to normal epithelium, but those of SHH, SMO and GLI1 were not.

shown). Expression of SHH and PTCH1 molecules in cancer tissue could be practically divided into the two types including focal and diffuse types (fig. 1). Differentiated type of cancer (n = 16) included 4 focal SHH and 11 focal PTCH1 expression. Undifferentiated type of cancer (n = 25) included 16 focal SHH and 19 focal PTCH1 expression.

Correlation between the Expression of SHH Signaling Pathway Molecules mRNA and Clinicopathological Parameters in Patients with Gastric Cancer

PTCH1 mRNA levels were significantly higher in cancer tissue compared to normal epithelium, but levels of *SHH*, *SMO* and *GLI1* mRNA were not significantly different between these tissues (fig. 2).

We performed RQ-PCR to investigate the correlation between the expression levels of the *SHH* signaling pathway components, *SHH*, *PTCH1*, *SMO* or *GLI1* and clinicopathological factors (table 2). Expression of *SHH* was not significantly correlated with any clinicopathological factors. Expression of *PTCH1* was significantly correlated with tumor differentiation, stromal quantity, and cytology of the peritoneal surface. Expression of *SMO* was significantly correlated with age, stromal quantity and peritoneal metastasis. Expression of *GLI1* was significantly correlated with age, tumor differentiation, stromal quantity and the conclusive stage. Together, these data suggest that significant upregulation of *SHH* pathway target molecules occurs in association with criteria indicating tumor progression. Expression of *SMO* and *GLI1* in older patients (>60 years) tended to be lower than in younger patients, who all had undifferentiated types of gastric cancer.

We compared the expression of SHH pathway molecules with each other and found that there were significant correlations between the expression of *SHH* and *PTCH1* and between the expression of *PTCH1* and all of the other pathway molecules investigated. There was also a significant correlation between the expression of *SMO* and *GLI1* (table 3).

Prognostic Value of SHH Signaling Molecule Expression Levels in Patients with Gastric Cancer

Relapses occurred in 8 patients who received curative surgery due to the recurrence of peritoneal metastasis (n = 5), hepatic metastasis (n = 2) and lymph node metastasis (n = 1). Causes of death in patients, including noncurative operation cases, were peritoneal metastasis (n = 7), hepatic metastasis (n = 3), and other diseases (n = 1). Patients who underwent noncurative surgery received postoperative chemotherapy using S-1, cisplatin, paclitaxel or irinotecan, according to the choice of the physician.

To determine correlations between the expressions of *SHH*, *PTCH1*, *SMO* and *GLI1* and patient prognosis, pa-